EFFECT OF SELF-HEALING ON THE CHLORIDE DIFFUSIVITY AT EARLY AGE

K Olivier, A. Darquennes, F. Benboudjema, R Gagné

EFFECT OF SELF-HEALING ON THE CHLORIDE DIFFUSIVITY AT EARLY AGE

K. Olivier[1,2], A. Darquennes[1], F. Benboudjema[1] and R. Gagné[2]

[1]LMT (ENS Cachan, CNRS, Université Paris Saclay), 94235 Cachan, France (kelly.olivier@ens-cachan.fr, aveline.darquennes@ens-cachan.fr, farid.benboudjema@ens-cachan.fr)
[2]Centre de recherche sur les infrastructures en béton (CRIB), Université de Sherbrooke, Québec, Canada (Richard.Gagne@usherbrooke.ca)

ABSTRACT

The chloride diffusivity of cementitious materials significantly affects the durability of civil engineering structures (e.g. reinforced concrete buildings) and the waste containment matrices (e.g. sediments, radioactive waste). Its influence becomes greater when cracks appear due to restrained shrinkage. The results of an experimental campaign on the chloride diffusion characteristics of uncracked, cracked and self-healed mortar specimens are presented at several ages. The mortar compositions are characterized by several contents of blast-furnace slag. The diffusion characteristics are measured by means of accelerated migration tests and solutions titration with silver nitrate to determine the steady state stage and the effective diffusion coefficient. The cracking size is monitored using optical microscopy. Results clearly show that self-healing is a positive phenomenon that limits and reduces the crack size, therefore leading to a decrease of the diffusion coefficient. Moreover, the addition of blast-furnace slag intensifies this trend due to the slow hydration kinetics of this type of hydraulic binder.

Keywords: Blast-furnace slag, Cracking, Diffusion, Migration test, Self-healing

Aveline Darquennes, Assistant Professor
Ecole Normale Supérieure de Cachan
Civil Engineering Department
61 avenue du Président Wilson
94235 Cachan
France

Email: aveline.darquennes@ens-cachan.fr
Tel: +33 (0)1 47 40 53 69

1. INTRODUCTION

A major pathology affecting reinforced concrete structures is the corrosion of steel reinforcement due to carbonation and chloride diffusion. This deterioration is amplified when concrete cover is cracked [1, 2]. In marine environment, concrete made with Ground Granulated Blast-Furnace-Slag (GGBFS) cement is often used for civil engineering structures as it offers many advantages such as reclamation of industrial wastes, decreased CO_2 emissions produced during the clinkerization process in cement manufacturing (by limiting the clinker content in the cementitious material) and enhanced material properties such as workability and long-term compressive strength [3, 4]. Given the low heat release, this type of cementitious material is recommended for massive structures such as dams and bridges. Nevertheless, several civil engineering structures made with GGBFS cement presented cracking at early age due to restrained shrinkage [5, 6]. This cracking reduces the mechanical properties and leads to an increased penetration risk by aggressive agents such as CO_2 and chloride. Structures made with GGBFS cement showed however evidence of self-healing of cracks that seems to be related to the hydration of anhydrous particles at early age (GGBFS, clinker) [7, 8] and/or calcite formation due to portlandite carbonation on the long term [9, 10].

In this study, experimental investigations are performed to analyze the effect of a traversing crack obtained by splitting tests on the chloride diffusion in steady-state conditions and the effect of self-healing. Three mortar compositions characterized by different blast-furnace slag contents are studied at early age by means of an accelerated migration test under an electrical field.

2. EXPERIMENTATION PROCEDURE

2.1. Materials

Three mortar compositions are studied in this experimental campaign: a Portland cement mortar (CEMI 52.5 N CP2), a slag cement mortar (CEM III/A 52,5 L PM-ES-CP1) and a blended mortar with 50% Portland cement (CEMI 52.5 N CP2) and 50% ground granulated blast-furnace slag (GGBFS) (volumic substitution). They are referred hereafter as CEMI, CEMIIIA and 50GGBS respectively. The content of GGBFS for the slag cement CEM III/A is equal to 60% (mass percentage). The clinker and ground granulated blast-furnace slag are of the same origin. The chemical composition of these components is given in Table 1.

Table 1. Chemical composition

Oxides (%)	CEMI	CEMIIIA	GGBFS
CaO	65.9	49.9	42.7
SiO_2	20.8	29.1	36.7
Al_2O_3	5.4	8.5	11.3
MgO	1.1	5.0	7.0
SO_3	3.4	2.67	0.2

Table 2. Mortar composition (kg/m^3)

	CEMI	CEMIIIA	50GGBS
Cement	563	563	281
GGBFS	/	/	258
Water	281		
Sand	1409		

Details on the mortar compositions are given in Table 2. Their water/binder (W/B) ratios are equal to 0.50 for the first two compositions and 0.52 for the third one. The paste volume, a parameter affecting

the shrinkage evolution, is kept constant for all mortar compositions. The same normalized siliceous sand is used.

2.2. Testing procedure

The effective chloride diffusion coefficient was determined by chloride migration under accelerated and steady-state conditions. Cylindrical specimens (diameter Ø = 110 mm, height h = 220 mm) were made for all compositions. After mixing, the specimens were stored in a room at 23°C ± 1°C and 45% ± 5% relative humidity (R.H.). The molds were removed after 2 days and the specimens stored under water for 4 days in a room at 23°C ± 1°C. At the 6th day, 3 cylindrical disks (h = 30 mm) were sawn from the specimens. Each disk was confined in a two-component resin reinforced with glass fibers and then cracked by means of a splitting test at 7 days. The crack width was measured with an optical microscope. One specimen was tested immediately; the others were stored for 14 or 21 days under tap water in individual boxes. Before the diffusion test, the specimens were saturated by hydroxide-sodium solution (0.3 mol/l) for 24 hours. An uncracked specimen was tested for each composition at 7 days.

For the chloride diffusion testing, a mortar specimen was placed between two cells and an electrical potential difference of 10 V was maintained across the specimen ends (Figure 1). The upstream cell was filled with a sodium-chloride solution (0.7 mol/l). The anodic solution corresponds to seawater concentration. The downstream cell was filled with a sodium-hydroxide solution (0.3 mol/l). The cathode solution is close to the interstitial solution concentration. The test lasted 7 days. Temperature was measured in one cell with a thermocouple. The solutions in the cells were removed every 12 hours and the chloride ions content of the downstream cell was quantified by titration according to the Charpentier-Volhard method described hereafter.

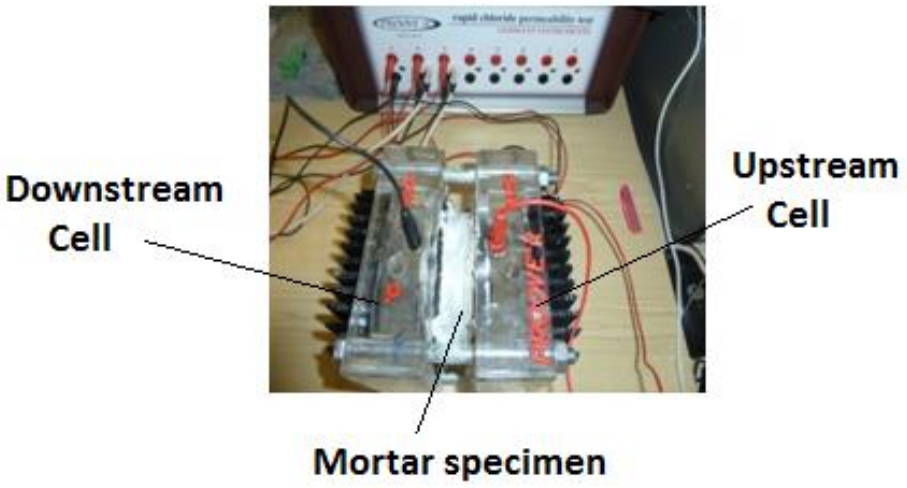

Figure 1. Accelerated chloride diffusion testing.

An important amount of silver nitrate ($AgNO_3$) is first added to the solution. The Ag ions react with the available chloride ions and the surplus is determined by adding potassium thyocyanate (KSCN) at the end the chemical reaction (a). The end of this reaction is determined with iron oxide (Fe_2O_3), leading to the formation of a red iron thyocyanate precipitate ($Fe(SCN)_3$) subsequent to the chemical reaction (b). Note that nitric acid was initially added to avoid the formation of metallic hydroxide.

$$Ag^+ + SCN^- \leftrightarrow AgSCN \quad \text{(a)}$$

$$Fe^{3+} + 3SCN^- \leftrightarrow Fe(SCN)_3 \quad \text{(b)}$$

During the accelerated migration test, the ions migration is primarily due to the electrical field. The diffusion coefficient is determined with Equation (1):

$$D_{eff} = \frac{R*T*h*J_c}{z*F*U*C_a} \quad (1)$$

where R is the gas constant (8.314 J/mol K), T the temperature (K), h the specimen height (m), z the chloride valence (1), F the Faraday constant (96500 J/V mol), U the differential potential (V), C_a the anodic solution concentration (mol/m^3) and J_c the effective flux (mol/m^2 s^1). This last parameter is computed with Equation (2).

$$J_c = \frac{V*\Delta C}{A*\Delta t} \quad (2)$$

where V is the cell volume (l), ΔC the differential concentration (mol/l), A the exposed specimen area (m^2), and Δt the time increment (s).

3. EXPERIMENTAL RESULTS AND DISCUSSION

3.1. Chloride concentration evolution and diffusion coefficient

The chloride concentration evolution in the downstream cell is presented in Figure 2. For all the specimens, initially the concentration slowly increases. During this first stage, chloride ions migrate through saturated pores in the mortar specimen but they do not yet reach the downstream cell. After 3 days, the concentration rate significantly increases and becomes constant (steady-state condition) leading to a constant chloride ions flux. The beginning of this second stage depends on the mortar porosity and the chloride binding capacity of the cementitious matrix [11]. These results are in agreement with [1, 12].

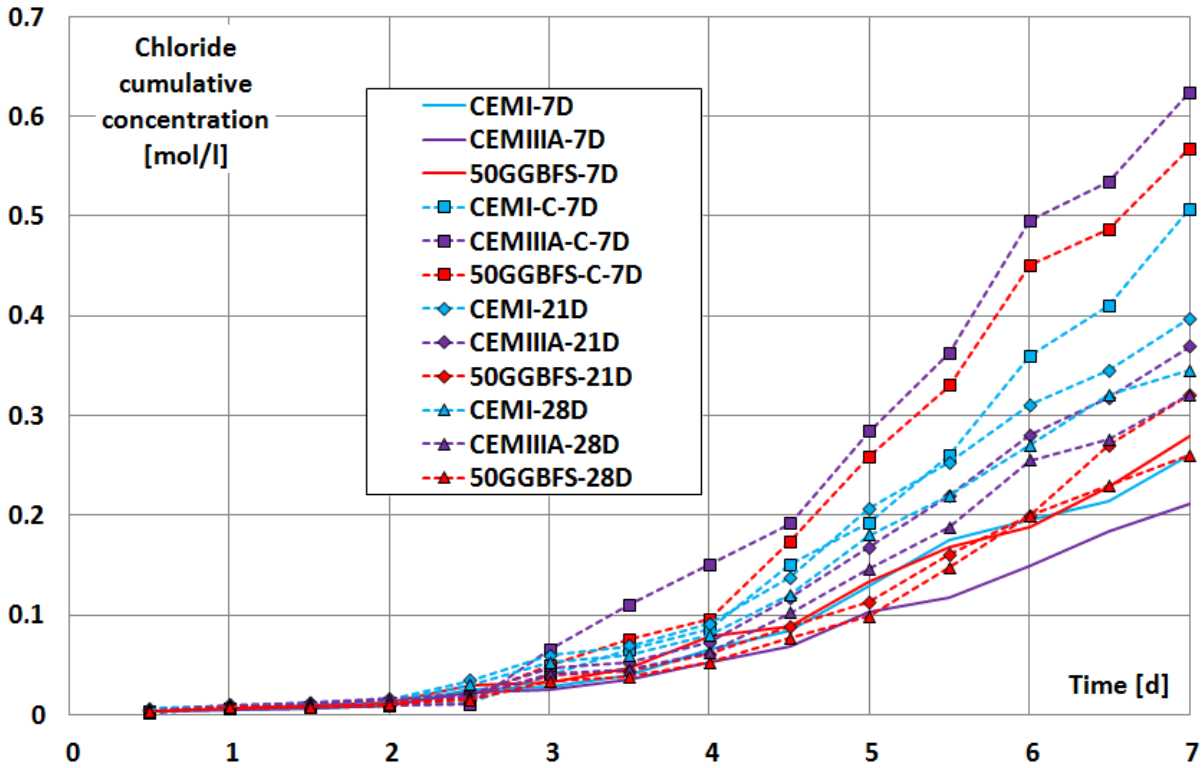

Figure 2. Chloride cumulative concentration for 7 days old uncracked (7D) and 7 days old freshly-cracked (C-7D) specimens, and 21 days old (21D) and 28 days old (28D) self-healing specimens.

The difference on the behavior of the uncracked specimens is directly related to the paste matrix properties. The lower final chloride concentration (Figure 2) and the effective diffusion coefficient

(Figure 3) of CEMIIIA is linked to its lower connected porosity [13] related to the formation of additional C-S-H. The higher value for 50GGBFS can be linked to its slow hydration kinetics leading to a higher connected porosity at early age [14]. After cracking, the final value and the evolution rate of the chloride concentration (Table 3) in the downstream cell under steady-state conditions are significantly increased for all the compositions. They are directly proportional to the average specimen crack width. Nevertheless, self-healing strongly decreases the final value and the evolution rate of the chloride ions concentration, particularly after the first 14th curing days. Moreover, these parameters are lower for the specimens containing blast-furnace slag (CEMIIIA and 50GGBFS) despite an initial wider crack. It seems therefore that these compositions are characterized by a greater self-healing capacity. Indeed, these trends reveal the presence of new products inside the cracks that narrow the crack widths and improve the chloride migration resistance of the material. This is confirmed by the average crack width evolution (Table 3). At 28 days, the evolution of chloride concentration for 50GGBFS is very close to that of the respective uncracked specimen. This last observation suggests that the self-healed 50GGBFS matrix is characterized by similar transfer properties as the respective uncracked matrix.

Table 3. Width of the initial and healed crack – Chloride concentration rate in steady state

	CEMI			CEMIIIA			50GGBFS		
	Initial crack width (µm)	Crack width after healing (µm)	Concentration rate (10^{-3} mol/l* day)	Initial crack width (µm)	Crack width after healing (µm)	Concentration rate (10^{-3} mol/ l* day)	Initial crack width (µm)	Crack width after healing (µm)	Concentration rate (10^{-3} mol/ l* day)
7D	/	/	75	/	/	61	/	/	71
C7D	126	/	161	152	/	185	143	/	185
21D	131	43	113	161	48	112	138	26	101
28D	137	41	101	168	44	97	148	22	83

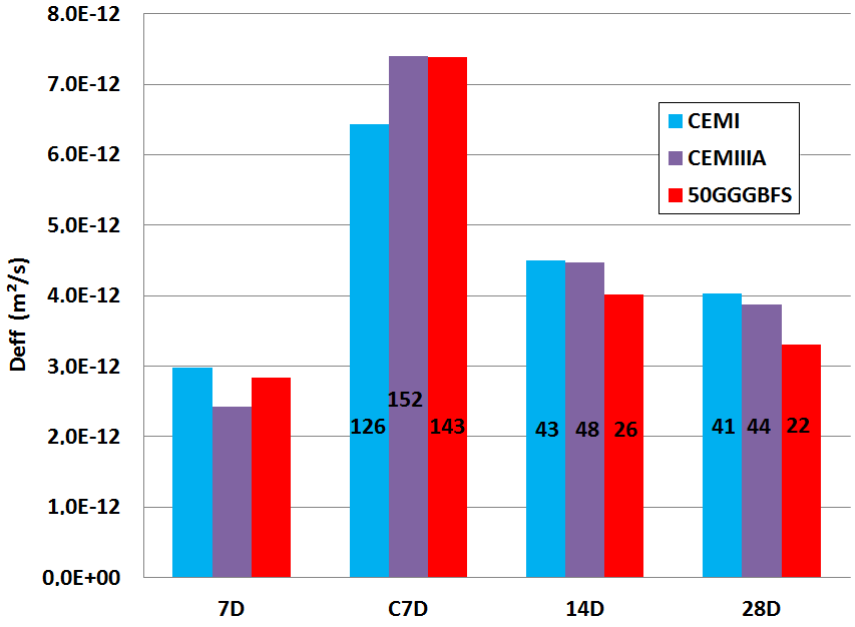

Figure 2. Diffusion coefficients and crack widths for all compositions

The slope of the curve for the final linear segment (Figure 2) is used to calculate the effective diffusion coefficient of chloride (Figure 3) using equations 1 and 2. Similar trends with the diffusion coefficient are observed. The uncracked specimens exhibit the lowest diffusion coefficients (2.99 10^{-12} m²/s, 2.43 10^{-12} m²/s and 2.84 10^{-12} m²/s for CEMI, CEMIIIA and 50GGBFS respectively). Despite a lower diffusion coefficient for uncraked mortar, CEMIIIA is characterized by a larger chloride diffusion (7.4 10^{-12} m²/s) after cracking. This is directly related to its larger crack width (153 µm). A

significant increase of this parameter is also observed for the other compositions. Indeed, the value of the diffusion coefficient of the cracked specimens increased by 115%, 148% and 147% for CEMI, CEMIIIA and 50GGBFS respectively. After twenty-one days under water curing, this parameter decreases by 37%, 40% and 49% for CEMI, CEMIIIA and 50GGBFS respectively. These observations confirm the positive role of self-healing on the chloride migration intensity and kinetics, particularly for mortars containing blast-furnace slag. These results are related to the reaction potential of blast-furnace slag. Indeed, the hydration degree of mortars containing blast-furnace slag is lower at 7 days [15]. It should be noted that the kinetics of self-healing is more important during the first 14 days under water for all the compositions. Finally, the results obtained with the chloride diffusion test confirm the potential of this method to monitor self-healing as suggested by [23, 24], particularly for cementitious materials with mineral additions.

3.2. Relation between crack size and diffusion coefficient

Figure 3 presents the effective diffusion coefficients ratio for the cracked and the uncracked specimens as function of the crack width. A linear behavior is observed for all the compositions. Similar observations are mentioned for ordinary and high-performance concretes [1]. This ratio is slightly higher for mortars with blast-furnace slag (CEMIIIA and 50GGBFS). This can be explained by the lower migration/matrix interaction of chloride ions in the perpendicular direction to the crack due to their denser cementitious matrix. This is in accordance with the lower diffusion coefficient for their respective uncracked specimen (Figure 2).

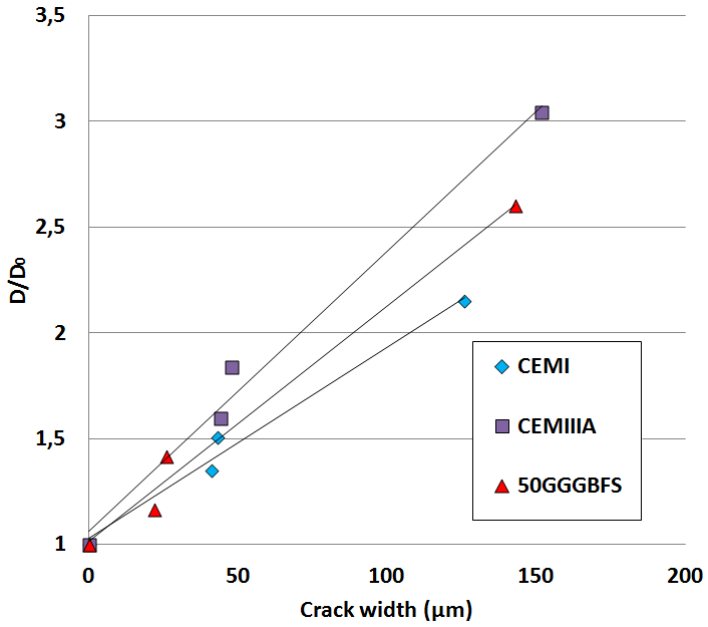

Figure 3. Evolution of the D/D_0 ratio as function of the crack width (D_0 = the effective diffusion coefficient of the uncracked specimen).

3.3. Comparison between the theoretical and experimental diffusion coefficients

To determine the effect of crack width on the chloride penetration, Equation 3 is used to estimate a theoretical diffusion coefficient (D_{theo}). In this relation, the crack is considered delimited by two parallel planes perpendicular to the specimen extremities [2].

$$D_{theo} = \frac{A_c D_f + A_{un} D_{un}}{A_c + A_{un}} \quad (3)$$

where A_c is the area of the crack (m²), A_{un} the uncracked area of the specimen (m²), D_f and D_{un} are the chloride ions diffusion coefficient in the free solution ($2.032\ 10^{-9}$ m²/s) and of the uncracked material (m²/s) respectively.

In order to compare the theoretical and the experimental results, the diffusion coefficients are divided by the measured diffusion coefficient of the uncracked material in Table 4. It appears that the theoretical relation leads to an over- or underestimation of the diffusion coefficient of the chloride ions. The absolute error is sometimes significant (50GGGFS at 28 days, for example). Simplifying the crack by opting for a parallel model without considering roughness and tortuosity can explain these differences.

Table 4. Comparison between theoretical (Dtheo) and experimental (Dexp) diffusion coefficients

	CEMI			**CEMIIIA**			**50GGBFS**		
	D_{theo}/D_{un}	D_{exp}/D_{un}	Absolute error	D_{theo}/D_{un}	D_{exp}/D_{un}	Absolute error	D_{theo}/D_{un}	D_{exp}/D_{un}	Absolute error
C7D	2.0	2.2	0.08	3.3	3.0	0.09	3.8	2.6	0.45
21D	1.3	1.5	0.11	2.3	1.8	0.25	2.8	1.4	0.99
28D	1.3	1.4	0.02	2.3	1.6	0.42	2.8	1.2	1.39

4. CONCLUSIONS

This study focuses on the self-healing phenomenon in cementitious materials with different contents of blast-furnace slag. Chloride diffusion tests were used to better understand the effect of mineral additions on the kinetics of self-healing and to underline the benefit of GGBFS additions in accelerating and amplifying this phenomenon. The main results are summarized below:

- For uncracked specimens, the effective chloride diffusion coefficient is lower for mortar with blast-furnace slag.
- The chloride diffusion coefficient of cracked samples increases with increasing crack width. These two parameters are characterized by a linear relation for all the studied mortar compositions.
- The ratio of the diffusion coefficients for cracked and uncracked specimens is lower for the Portland cement mortar and it is less sensitive to the crack width. This can be explained by the more important interaction between the flow through the crack and the cementitious matrix (lower density).
- The chloride diffusion test is an efficient method to monitor the self-healing phenomenon for cementitious materials with mineral additions. It confirms that self-healing has a positive role in terms of durability.
- The self-healing kinetics of mortars stored under water evolves quickly during the first two weeks after cracking. The kinetics is faster for mortars with blast-furnace slag at early age, and it is directly related to the slow hydration degree evolution for this type of composition.

ACKNOWLEDGMENTS

The authors would like to thank Z. Djamai for his valuable contribution to the project.

REFERENCES

[1] Djerbi, A., Bonnet, S., Khelidj, A., & Baroghel-bouny, V. (2008). Influence of traversing crack on chloride diffusion into concrete. *Cement and Concrete Research*, 38, 877-883.

[2] Gérard, B., & Marchand, J. (2000). Influence of cracking on the diffusion properties of cement-based materials - Part I : Influence of continuous cracks on the steady-state regime. *Cement and Concrete Research*, 31, 37-43.

[3] Dubovoy, V. S., Gebler, S. H., Klieger, P., & Whiting, D. A. (1986). Effects of Ground Granulated Blast-Furnace Slags on Some Properties of Pastes, Mortars and Concrete, Blended Cements. *ASTM STP 897*, American Society for Testing and Materials, Philadelphia, 29-48.

[4] Itim, A., Ezziane, K., & Kadri, E. (2011). Compressive strength and shrinkage of mortar containing various amounts of mineral additions. *Construction and Buildings Materials*, 25, 3603-3609.

[5] Darquennes, A., Staquet, S., & Espion, B. (2011). Behaviour of slag cement concrete under restraint conditions. *European Journal of Environmental and Civil Engineering (EJECE)*, 15/7, 1017-1029.

[6] Briffaut, M., Benboudjema, F., D'Aloia, L., Bahrami, B., & Bonnet, A. (2012). Analysis of cracking due to shrinkage restraint in a concrete tunnel. *International Conference on Numerical Modeling Strategies for Sustainable Concrete Structure*, May 29 – June 1, Aix-en-Provence, France.

[7] Hearn, N. (1998). Self-sealing, autogenous healing and continued hydration : What is the difference ? *Materials and structures*, 31, 563-567.

[8] Ter Heide, N. (2005). Crack healing in hydrating concrete. *Master Thesis*, Delft Technical University , The Nederlands.

[9] Clear, C.A. (1985). The effects of autogenous healing upon the leakage of water through cracks in concrete, *Technical report 559.*

[10] Gagné, R., Argouges, M. (2012) A study of the natural self-healing of mortars using air-flow measurements, *Materials & Structures*. 45, 1625-1638.

[11] Truc, O. (2000). A new way for determining the chloride diffusion coefficient in concrete from steady state diffusion test. *Cement and Concrete Research*, 30, 217-226.

[12] Jang, S.Y., Kim, B. S., & Oh, B. H. (2011). Effect of crack width on chloride diffusion coefficients of concrete by steady-state migration tests. *Cement and Concrete Research*, 41, 9-19.

[13] Darquennes, A., Staquet, S., Delplancke-Ogletree, M.-P. & Espion, B. (2011). Effect of autogenous deformation on the cracking risk of slag cement concretes. *Cement and Concrete Composites*, 33, 368-379.

[14] Darquennes, A., Rozière, E., Khokhar, M.I.A., Turcry, P., Loukili, A., & Grondin, F. (2012). Long term deformations and cracking risk of concrete with high content of mineral additions, Materials and Structures, *45(11)*, 1705-1716.

[15] Olivier, K., Darquennes, A., Benboudjema, F., & Gagné, R**. (**2013). Impact de l'ajout de laitier de haut-fourneau sur l'auto-cicatrisation des matériaux cimentaires**.** *14ème Edition des journées scientifiques du Regroupement francophone pour la recherche et la formation sur le béton (RF)²B*, Août, Sherbrooke, Canada.

[16] Termkhajornkit, P., Nawa, T., Yamashiro, Y., & Saito, T. (2009). Self-healing ability of fly ash-cement systems. *Cement and Concrete Composites*, 31, 195-203.

[17] Jacobsen, S., Marchand, J., & Boisvert, L. (1996). Effect of cracking and healing on chloride transport in OPC concrete. *Cement and Concrete Research*, 26. (6), 869-881.